MADRID
inter.noise 2019
June 16 - 19
NOISE CONTROL FOR A BETTER ENVIRONMENT

Predicting the Attenuation Characteristics of a Micro-vibration Damper for Automobile Bodies using Transfer-function Synthesis

Nakamura, Hiroki[1]
Kanagawa University
3-27-1, Rokkakubasi, Kanagawa-ku, Yokohama, Japan

Watanabe, Ryota[1]
Kanagawa University

Kamo, Toshiaki[2]
Yamaha Motor Co., Ltd
2500 Shingai, Iwata, Shizuoka, Japan

Hayakawa, Norikuni[2]
Yamaha Motor Co., Ltd

Iikura, Masahiko[2]
Yamaha Motor Co., Ltd

Yamazaki, Toru[1]
Kanagawa University

ABSTRACT

A test damper developed to suppress the micro-vibrations of automobile bodies can produce a velocity-independent and nearly constant high damping force even at very small speeds. To select the optimum damping force for an arbitrary vehicle, it is necessary to establish a method for predicting the vehicle vibrations when the damper is installed, and this requires a physical model of the damper itself. A previous report elucidated the mechanism by which the damping force is generated and a linearization method is described.

In the present report, a method is proposed for estimating the vibration response; the vibration of the vehicle body when the target linear damper is installed is estimated using only the vibration response; the transfer functions among the input, evaluation, and coupling points on the vehicle body; and the transfer function of the target damper itself. The feasibility of the proposed method is examined using finite-element simulation of a mock-up frame and a test damper.

[1] hiroki-nak@kanagawa-u.ac.jp
[2] kamoto@yamaha-motor.co.jp

From the results, the vibration response of the mock-up frame with the test damper estimated with the proposed method and that calculated by direct analysis match well. Furthermore, application to an actual vehicle experiment is considered by estimating the response to a multi-directional and multi-point input.

Keywords: Vibration, Dynamic model, Transfer-function synthesis, Micro-vibration damping
I-INCE Classification of Subject Number: 76

1. INTRODUCTION

There is a pressing need to reduce the vibrations of automobile frames for better performance, maneuverability, and comfort. However, conventional viscous dampers do not perform this task well because automobile-frame vibrations have very small amplitudes. Instead, a nonlinear damper (known as a performance damper) has been developed to suppress the micro-vibrations of automobile bodies; it uses an oil-filled hydraulic pressure-control valve to generate a velocity-independent and nearly constant damping force [1].

The aim of the present study is to optimize the design of the best-performing damper for an arbitrary vehicle to achieve better performance and comfort. To do so, it is necessary to construct a model of the target damper itself and to establish a method for estimating the vibration response when the device (or a target damper) is coupled with the main structure (an automobile frame). A previous study [2,3] considered the modeling of the target damper itself. In [2], the mechanism for generating the damping force with the pressure-control valve and a kinematic model (nonlinear characteristics) was constructed under quasi-static conditions, and a linearized model of the damping force under sinusoidal excitation was constructed based on the describing-function method. The validity of the proposed model under quasi-static conditions (low frequency) was shown through theoretical and experimental analysis. In [3], a more precise model of how the damping force varies with the piston speed was reported considering the response delay of each component, which is appropriate for the dynamic state.

In this report, a method is proposed for estimating the vibration response when a target nonlinear damper is installed on an automobile frame. In particular, the method of transfer-function synthesis is used. Transfer-function synthesis is an effective tool for estimating the vibration response of a coupled system of two or more subsystems from the frequency characteristics of each subsystem and the coupling stiffness among the subsystems. Herein, transfer-function synthesis is used to estimate the vibration response of an automobile frame attached to a test nonlinear damper. Specifically, having either simulated or measured the compliance (i.e., the vibration displacement divided by the input force) at an evaluation point and coupling points on a mock-up frame and a test damper, the vibration response of the evaluation point when the test damper is attached is estimated. In addition, because each transfer function can be derived from either an experiment or a simulation, this is an effective tool in terms of practical utilization. Also, because the sharing of information among companies can be limited, another advantage of this method is that it makes it easy for car manufacturers and suppliers to collaborate.

First, the methodology of transfer-function synthesis and the calculation method for a nonlinear damper are described. In particular, the target test damper responds nonlinearly to the vibration displacement, meaning that an equivalent damping coefficient cannot be calculated definitively. An iterative calculation method is then proposed for evaluating the vibration response, and a preliminary simulation is conducted using the finite-element method (FEM); a linear damper (subsystem B) is attached to a mock-up frame (subsystem A), and the vibration response of the entire system is estimated using transfer-function synthesis. Direct analysis of the entire system by FEM is considered to give the true values against which the estimated values are compared to assess the feasibility. A simulation with a nonlinear damper on a mock-up frame is then performed, and a full-scale experiment is considered. Several conditions are also discussed, such as the direction of the input force, multiple inputs, and the installation of multiple test dampers.

2. METHODOLOGY

2.1. Transfer-function Synthesis

Transfer-function synthesis is a calculation method that estimates the vibration response of an arbitrary structure (subsystem A) when another substructure (subsystem B) is attached. Specifically, the transfer function of the entire system is calculated from several vibration responses, namely, the compliances of an evaluation point and coupling point(s) on subsystem A for the forces on the vibration source and coupling points, the compliances of subsystem B on the coupling point(s), and the stiffness of the coupling point(s). The calculation load is relatively small compared to direct calculation of the full model. Figure 1 shows the model in which a test damper (subsystem B) is coupled at two points on a mock up frame (subsystem A or main system).

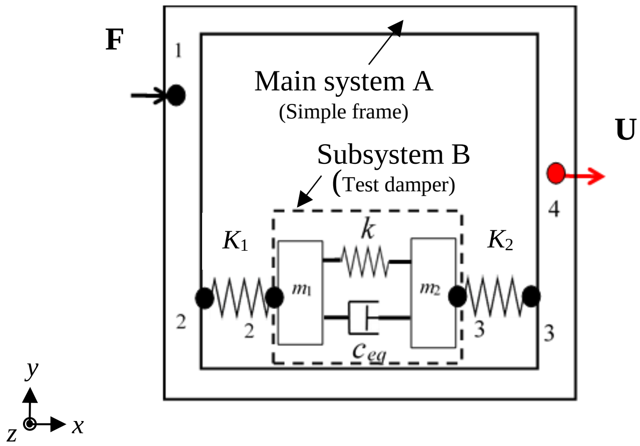

Figure 1 Dynamic model of simplified frame and test damper

In this figure, point 1 is the input to the main system, points 2 and 3 are the coupling points of the main system and subsystem B, and point 4 is the evaluation point on the main system. The input force vector and the displacement vector at the evaluation point are defined as **F** and **U**, respectively. The correlation between vibration response U_4^A and input F_1^A is expressed as

$$\mathbf{U}_4^A = \mathbf{G}_{41}^A \mathbf{F}_1^A + \mathbf{G}_{42}^A \mathbf{g}_2^A + \mathbf{G}_{43}^A \mathbf{g}_3^A \, , \tag{1}$$

where $\mathbf{G}_{ij}{}^A$ is the compliance of #i for input on #j, **g** is the transmitted force vector at the coupling point. The transmitted force **g** is defined as follows based on Hooke's law:

$$\mathbf{g}_2^A = \mathbf{K}_1 \left(\mathbf{U}_2^B - \mathbf{U}_2^A \right), \tag{2}$$

$$\mathbf{g}_3^A = \mathbf{K}_2 \left(\mathbf{U}_3^B - \mathbf{U}_3^A \right), \tag{3}$$

where U_2^A, U_3^A, U_2^B, and U_3^B are the displacements of points 2 and 3 on subsystems; **K** is the stiffness vector between subsystems A and B. A and B and can also be expressed as follows with the input force and transfer functions:

$$\mathbf{U}_2^{\mathrm{A}} = \mathbf{G}_{21}^{\mathrm{A}}\mathbf{F}_1^{\mathrm{A}} + \mathbf{G}_{22}^{\mathrm{A}}\mathbf{g}_2^{\mathrm{A}} + \mathbf{G}_{23}^{\mathrm{A}}\mathbf{g}_3^{\mathrm{A}} , \tag{4}$$

$$\mathbf{U}_3^{\mathrm{A}} = \mathbf{G}_{31}^{\mathrm{A}}\mathbf{F}_1^{\mathrm{A}} + \mathbf{G}_{32}^{\mathrm{A}}\mathbf{g}_2^{\mathrm{A}} + \mathbf{G}_{33}^{\mathrm{A}}\mathbf{g}_3^{\mathrm{A}} , \tag{5}$$

$$\mathbf{U}_2^{\mathrm{B}} = \mathbf{G}_{22}^{\mathrm{B}}\mathbf{g}_2^{\mathrm{B}} + \mathbf{G}_{23}^{\mathrm{B}}\mathbf{g}_3^{\mathrm{B}} , \tag{6}$$

$$\mathbf{U}_3^{\mathrm{B}} = \mathbf{G}_{32}^{\mathrm{B}}\mathbf{g}_2^{\mathrm{B}} + \mathbf{G}_{33}^{\mathrm{B}}\mathbf{g}_3^{\mathrm{B}} . \tag{7}$$

The transmitted forces $\mathbf{g}_2^A$ and $\mathbf{g}_3^A$ are then determined as

$$\begin{bmatrix} \mathbf{g}_2^{\mathrm{A}} \\ \mathbf{g}_3^{\mathrm{A}} \end{bmatrix} = \begin{bmatrix} \mathbf{K}_1^{-1} + \mathbf{G}_{22}^{\mathrm{A}} + \mathbf{G}_{22}^{\mathrm{B}} & \mathbf{G}_{23}^{\mathrm{A}} + \mathbf{G}_{23}^{\mathrm{B}} \\ \mathbf{G}_{32}^{\mathrm{A}} + \mathbf{G}_{32}^{\mathrm{B}} & \mathbf{K}_2^{-1} + \mathbf{G}_{33}^{\mathrm{A}} + \mathbf{G}_{33}^{\mathrm{B}} \end{bmatrix}^{-1} \begin{bmatrix} -\mathbf{G}_{21}^{\mathrm{A}} \\ -\mathbf{G}_{31}^{\mathrm{A}} \end{bmatrix} \mathbf{F}_1^{\mathrm{A}} \tag{8}$$

by substituting Equations (4)–(7) for Equations (2) and (3). This suggests that $\mathbf{g}_2^A$ and $\mathbf{g}_3^A$ can be derived from the compliance, coupling stiffness, and input force. Here, the compliance **G** can be determined by either experiment or simulation.

2.2. Linearization of Target Nonlinear Damper

As described previously [2], the damping force F under quasi-static conditions comprises (i) the constant resistive force F_0 due to the cracking pressure of the pressure-control valve and the pressure override, and Equation (9) is derived by considering the direction of this resistive force. If the force due to the pressure override (the second term in Equation (9)) is approximately proportional to the piston speed (in other words, proportional to the flow rate through the valve), then we have

$$F = \mathrm{sgn}\left(\frac{\mathrm{d}x}{\mathrm{d}t}\right)F_0 + \alpha\frac{\mathrm{d}x}{\mathrm{d}t} . \tag{9}$$

This equation is linearized using the describing-function method under the assumption of excitation with constant frequency ω and amplitude X_0, and the equivalent damping coefficient c_{eq} is derived as

$$c_{eq} = \frac{4F_0}{\pi X_0 \omega} + \alpha . \tag{10}$$

This model is used to estimate the vibration response of the mock-up automobile frame with the damper attached.

2.3. Method for Estimating Vibration Response with Nonlinear Damper Attached

The procedure is as follows. 1) For a given value of ω, take an arbitrary value of X_0 (or c_{eq}) and calculate the displacements of coupling points 2 and 3 and evaluation point

4. 2) Calculate the relative displacement between the two coupling points and compare it with X_0. 3) Iterate until the relative displacement and X_0 converge. 4) When the relative displacement and X_0 correspond, the displacement of evaluation point #4 is the estimated value.

3. PRELIMINARY SIMULATION WITH A LINEAR DAMPER ON A FRAME

To demonstrate the validity of the proposed method, the vibration response is estimated under the following conditions. A linear damper (subsystem B) is attached to a mock-up frame (subsystem A), and the vibration response of the entire system is estimated using transfer-function synthesis. Direct analysis of the entire system by FEM is considered to give the true values against which the estimated values are compared to assess the feasibility.

3.1. Mock-up Frame

As shown in Figure 1, the aim is to estimate the vibration response of a mock-up frame attached to a damper. The specifications of the mock-up frame are as follows. The frame has a hollow rectangular cross section whose outer size is 130 mm × 100 mm and whose thickness is 15 mm. The outer size of the frame is 4240 mm × 1770 mm, approximately the same size as that of an ordinary automobile frame. The damper is attached laterally to the longitudinal part of the frame at a distance of 110 mm from the back edge. Here, point 1 is the input to the main system, points 2 and 3 are the coupling points of the main system and subsystem B, point 4 is the evaluation point on the main system, m_1, m_2, and k are the masses of the cylinder, the piston rod, and a spring of the test damper, respectively, K_1 and K_2 are the coupling stiffnesses of points 2 and 3, respectively, F is the excitation input, and U is the output displacement. In this study, what is estimated is the vibration response of point 4 for the input force on point 1.

3.2. Conditions of Numerical Simulation

In this section, the validity of the method of transfer-function synthesis is examined. The transfer functions of the mock-up frame (subsystem A) are calculated with FEM, and the transfer function of subsystem B with constant coefficient c_{eq} = 200 kNs/m is derived theoretically. With these data, the vibration response of evaluation point 4 is estimated with transfer-function synthesis and compared with that from direct analysis. To simplify the discussion, a sinusoidal input force is applied in the x direction with an amplitude of 500 N and a frequency from 1 Hz to 200 Hz in increments of 0.1 Hz. Also, the coupling stiffnesses are taken to be $K_1 = K_2 = 10$ GN/m.

3.3. Results of Simulation with Linear Damper

The vibration displacement calculated using each method, namely, direct analysis of the entire system and estimation with transfer-function synthesis, is shown in Figure 2. Also, the vibration response of the mock-up frame without the damper is shown as a reference. The results show that the estimated response corresponds to that from direct analysis. Furthermore, the damper reduces drastically the resonances at several frequencies: the vibration is reduced by more than 10 dB at 30 Hz, 85 Hz, and 140 Hz. On the other hand, the vibration around 50 Hz, 120 Hz, and 195 Hz is not reduced. The mechanism for the damping effect is determined from the modal shape of the mock-up frame, the details of which are discussed in the following section 5.4.

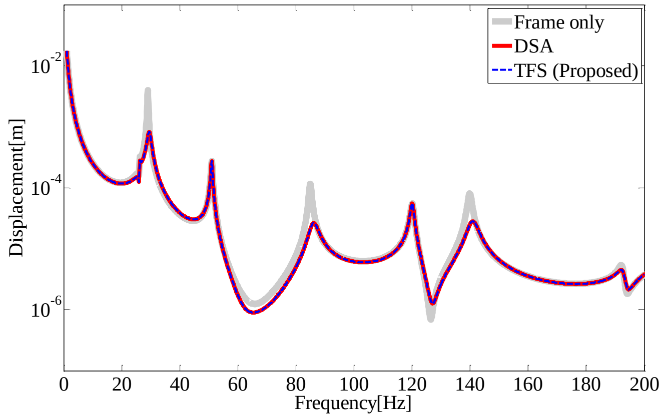

Figure 2 Comparison of displacement response in x direction for Transfer Function Synthesis (TFS), Direct Solution Analysis (DSA), and frame only (in the case of a linear damper)

4. SIMULATION WITH A NONLINEAR DAMPER ON A FRAME

The target test damper responds nonlinearly to the vibration displacement, meaning that the equivalent damping coefficient cannot be calculated definitively. Instead, c_{eq} is calculated iteratively until X_0 corresponds to the relative displacement of the two fastening points of the test damper, and the vibration response is estimated using the proposed model based on transfer-function synthesis (Equations (1)–(8)). To demonstrate the validity of the proposed method, the vibration response is estimated under the following conditions. A nonlinear damper (subsystem B) is attached to the mock-up frame (subsystem A), and the vibration response of the entire system is estimated with transfer-function synthesis. Direct analysis of the entire system by FEM is considered to give the true values against which the estimated values are compared to assess the feasibility.

4.1. Conditions of Numerical Simulation

The cracking pressure is assumed to create a damping force of $F_0 = 200$ N, and the process is iterated five times for each frequency (enough for convergence). Here, α in Equation (10) is relatively small and so is neglected ($\alpha = 0$). The other conditions are the same as those of the preliminary simulation in Section 3.

4.2. Results of Simulation with Nonlinear Damper

The vibration displacement calculated by each method, namely, direct analysis of the entire system and estimation with transfer-function synthesis, is shown in Figure 3. Also, the vibration response of the mock-up frame without the damper is shown as a reference. The results show that the estimated values correspond to those from direct analysis even when iteration considering the nonlinearity of the damper is applied. Compared with Figure 2, the reduction effect is relatively small (the reduction is now only approximately 0.2 dB). This is because the damping coefficient here is much smaller than that of the linear damper: the equivalent damping coefficient is 30 kNs/m at most, whereas the linear damping coefficient is 200 kNs/m. However, as shown later in section 5.1, the vibration response in the *z* direction is reduced very well. Furthermore, the proposed method calculates in 15 min whereas direct analysis takes 30 h, so the proposed method is much better in terms of the calculation load.

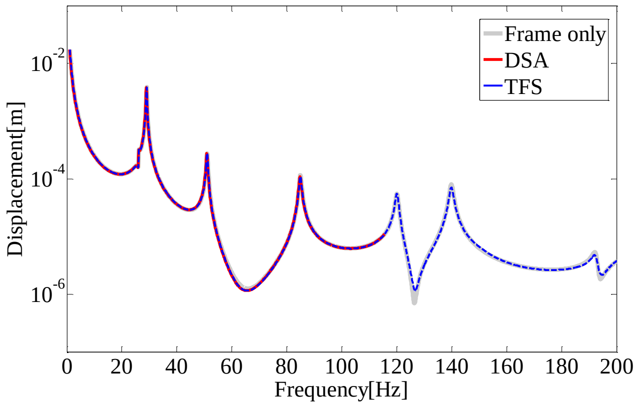

Figure 3 Comparison of displacement response for TFS, DSA, and frame only (in the case of a nonlinear damper)

5. DISCUSSION REGARDING PRACTICAL APPLICATION

In this section, several conditions are considered for practical application, such as experiments with an actual vehicle. In particular, a three-dimensional input force and multiple inputs are simulated.

5.1. Multi-directional Input Force

Here, a case is considered in which the excitation force acts in a direction other than that in which the damper moves. The orientation is shown in Figure 4. To simulate the vehicle being excited by road–tire interaction and the force being transmitted to the frame through the suspension, the excitation force acts in the x and z directions but the damping force acts in only the z direction. The damping force acting in the y direction could be modeled in the same way and so is omitted from this report.

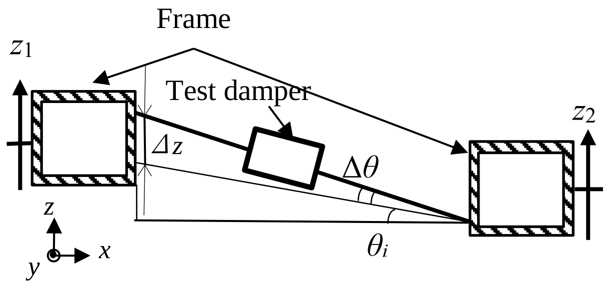

Figure 4 Schematic of vibration in z direction of test damper

5.2. Modeling of Damping Force in z Direction

A schematic of the vibrating mock-up frame around the coupling points in the z direction is shown in Figure 4. Here, θ_i is the initial tilt angle of the test-damper axis from the horizontal (x) axis, $\Delta\theta$ is the change of the tilting angle from the initial state, and z_1 and z_2 are the displacements of the coupling points on both sides. The slide Δx_z of the piston in the axial direction (approximately the x axis), which depends geometrically on the relative displacement in the z direction, is derived as follows with the assumption of $\Delta\theta << \theta_i$:

$$\Delta x_z \cong (z_1 - z_2)\theta_i \ . \tag{11}$$

Thus, the resistive force F_d acting axially on the piston and caused by the relative displacement in the z direction is expressed as follows with the equivalent damping coefficient c_{eqz}:

$$F_d = c_{eqz} \frac{d\Delta x_z}{dt} . \tag{12}$$

To simplify the discussion, α is considered to be approximately zero, and the equivalent damping coefficient c_{eqz} is derived as

$$c_{eqz} = \frac{4F_0}{\pi\omega X_{0.z}} , \tag{13}$$

where $X_{0.z}$ is the relative displacement in the x direction, which depends geometrically on the relative displacement in the z direction. Then, the following relation between the x direction and the z direction is derived:

$$X_{0.z} \cong |Z_{10} - Z_{20}|\theta_i \equiv Z_0\theta_i , \tag{14}$$

where Z_{10} and Z_{20} are the displacements of z_1 and z_2, respectively, for an arbitrary frequency, and Z_0 is the relative displacement amplitude between z_1 and z_2. Then, the damping force $F_{dz.1}$ acting in the z direction at the left-hand coupling point is expressed as

$$F_{dz.1} = -F_d \sin(\theta_i + \Delta\theta) . \tag{15}$$

The damping force $F_{dz.1}$ acting on point 2 is as follows with the approximation $\Delta\theta \ll \theta_i$:

$$F_{dz.1} = -\frac{4F_0}{\pi\omega Z_0}\theta_i \frac{d\Delta z}{dt} . \tag{16}$$

Likewise, the damping force $F_{dz.2}$ acting on point 3 (right-hand side) is $F_{dz.2} = -F_{d\,z.1}$.

5.3. Estimation of Vibration Response for Vertical Input Force

The vibration displacement when a two-dimensional excitation force $F_{x.z}$ is applied is calculated by each method, namely, direct analysis of the entire system and estimation with transfer-function synthesis. The results are shown in Figures 5 and 6 for the vibration responses in the z direction and the θ direction (direction of excitation force), respectively, where

$$F_{x.z} = \sqrt{F_x^2 + F_z^2}\, e^{j\theta} , \quad \theta = \tan^{-1}(F_z / F_x) . \tag{17}$$

Here, F_x and F_z are the x and z components of $F_{x.z}$, respectively, and θ is the direction of the excitation force. In this report, an example with F_x = 500 N and F_z = 1,000 N is simulated. To examine the difference due to the installed damper, two conditions are calculated, namely, F_0 = 200 N and F_0 = 800 N.

From Figure 5 and 6, the estimated values correspond to those from direct analysis, thereby supporting the feasibility of the proposed method. Also, the damping effect is more apparent in the θ direction (because of the vibration reduction in the z direction). Another feature is that more resonance frequencies (eight up to 100 Hz) are observed than in the previous case because modes now resonate in both the x and z directions. Furthermore, a difference due to F_0 is observed, suggesting that the proposed method is applicable to the optimal design of the target nonlinear damper.

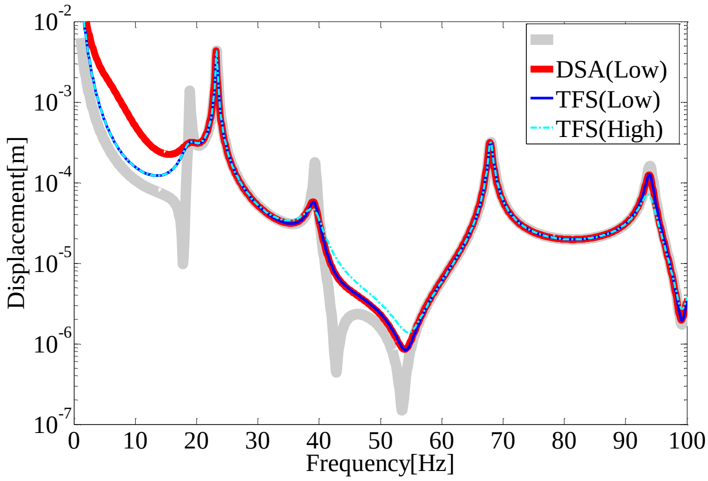

Figure 5 Comparison of displacement in z direction for TFS and DSA in the cases of F_0 are low and high

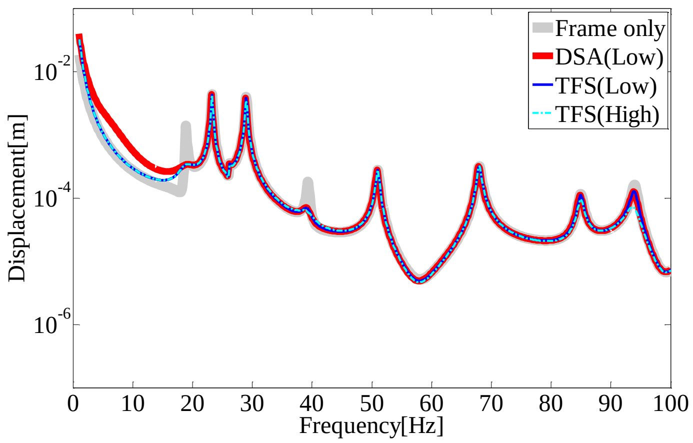

Figure 6 Comparison of displacement in θ direction for TFS and DSA in the cases of F_0 are low and high

5.4. Correlation Between Vibration Reduction and Modal Shape

The amount of attenuation is determined as

$$AT = 20\log\left[\frac{X_F}{X_d}\right]. \tag{19}$$

Tables 1 and 2 give the attenuation amounts for mode 1 (a representative frequency at which the damper had no effect) and mode 2 (a representative frequency at which the damper performed well), respectively. These results are compared with the following modal shapes.

Table 1 Resonance displacement in z direction and attenuation AT for mode 1

	Frame only	DSA (Low)	TFS (Low)
Frequency [Hz]	18.9	19.2	19.2
Displacement [mm]	1.40	0.37	0.38
AT [dB]		12.2	12.2

Table 2 Resonance displacement in z direction and attenuation AT for mode 2

	Frame only	DSA (Low)	TFS (Low)
Frequency [Hz]	23.3	23.2	23.3
Displacement [mm]	4.33	4.34	4.28
AT [dB]		-0.02	0.1

The modal shapes of modes 1 and 2 in the *yz* plane are shown in Figure 7(a) and (b), respectively. The longitudinal frame vibrates in opposite directions (antiphase) in mode 1 but in the same direction (in phase) in mode 2. The test damper is installed near the bottom of these figures, meaning that the relative displacement is large for mode 1 and small (or none) for mode 2. This means that the damper acts to reduce the vibration response when it slides more because of the relative displacement (or velocity).

(a) Mode 1 (antiphase)　　　　(b) Mode 2 (in phase)

Figure 7 Examples of mode shapes in yz plane

6. CONCLUSIONS

In this report, a method is proposed for estimating the vibration response when a target nonlinear damper is installed on an automobile frame. Specific remarks are as follows.

1) The vibration response of the evaluation point when the test damper is attached is estimated from the compliance (i.e., the vibration displacement divided by the input force) of the evaluation point and coupling points on a mock-up frame, and a test damper for input force is simulated. Also, the calculation is performed much faster than is direct analysis.

2) An iterative calculation method is used to deal with the nonlinearity of the test damper, allowing the vibration response to be estimated when a nonlinear damper is attached. How the modal shape influences the rate of vibration reduction is discussed.

3) A full-scale experiment is considered, and the influence of a multi-directional input force is demonstrated.

7. REFERENCE

1. S. Sawai, H. Okada, T. Kamo,
Development of Chassis Damping Technology by Hydraulic Damper, Proceedings of 2014 JSAE annual congress (spring), No.120-14 pp19-24, 2014 (In Japanese)
2. H. Nakamura, T. Kamo, H. Ohsawa, S. Fukushima, H. Sakanoue, T. Yamazaki
Modeling of an Attenuation Characteristics of the Damper Used for Micro Vibration of a Car Body, JSAE Transaction, No.47-6, pp.1367-1372, 2016 (In Japanese)
3. H. Nakamura, T. Kamo, H. Ohsawa, H. Sakanoue, T. Yamazaki
Modeling of an Attenuation Characteristics of the Damper Used for Micro Vibration of a Car Body 2nd report, JSAE Transaction, No.49-3, pp.611-616, 2018 (In Japanese)